

# Testosterone Antagonizes Doxorubicin-Induced Senescence of Cardiomyocytes

Paola Altieri, PhD; Chiara Barisione, PhD; Edoardo Lazzarini, PhD; Anna Garuti, PhD; Gian Paolo Bezante, MD; Marco Canepa, MD, PhD; Paolo Spallarossa, MD; Carlo Gabriele Tocchetti, MD, PhD; Sveva Bollini, PhD; Claudio Brunelli, MD; Pietro Ameri, MD, PhD

**Background**—Chronic cardiotoxicity is less common in male than in female patients receiving doxorubicin and other anthracyclines at puberty and adolescence. We hypothesized that this sex difference might be secondary to distinct activities of sex hormones on cardiomyocyte senescence, which is thought to be central to the development of long-term anthracycline cardiomyopathy.

**Methods and Results**—H9c2 cells and neonatal mouse cardiomyocytes were exposed to doxorubicin with or without prior incubation with testosterone or 17 $\beta$ -estradiol, the main androgen and estrogen, respectively. Testosterone, but not 17 $\beta$ -estradiol, counteracted doxorubicin-elicited senescence. Downregulation of telomere binding factor 2, which has been pinpointed previously as being pivotal to doxorubicin-induced senescence, was also prevented by testosterone, as were p53 phosphorylation and accumulation. Pretreatment with the androgen receptor antagonist flutamide, the phosphatidylinositol 3 kinase inhibitor LY294002, and the nitric oxide synthase inhibitor L-NG-nitroarginine methyl ester abrogated the reduction in senescence and the normalization of telomere binding factor 2 levels attained by testosterone. Consistently, testosterone enhanced the phosphorylation of AKT and nitric oxide synthase 3. In H9c2 cells, doxorubicin-stimulated senescence was still observed up to 21 days after treatment and increased further when cells were rechallenged with doxorubicin 14 days after the first exposure to mimic the schedule of anthracycline-containing chemotherapy. Remarkably, these effects were also inhibited by testosterone.

**Conclusions**—Testosterone protects cardiomyocytes against senescence caused by doxorubicin at least in part by modulating telomere binding factor 2 via a pathway involving the androgen receptor, phosphatidylinositol 3 kinase, AKT, and nitric oxide synthase 3. This is a potential mechanism by which pubescent and adolescent boys are less prone to chronic anthracycline cardiotoxicity than girls. (*J Am Heart Assoc.* 2016;5:e002383 doi: 10.1161/JAHA.115.002383)

**Key Words:** cardiotoxicity • doxorubicin • senescence • sex • testosterone

Anthracyclines are chemotherapeutic drugs used to treat several solid and hematological malignancies. A major dose-limiting side effect of these compounds is cardiac toxicity, which most often presents as subclinical myocardial dysfunction or overt heart failure toward the end of chemotherapy or later on, even after many years.<sup>1</sup> This

delayed form of anthracycline cardiotoxicity is referred to as chronic and has complex pathogenesis.<sup>2,3</sup> It has been shown recently that anthracyclines cause senescence of cardiomyocytes.<sup>4</sup> This event is central to the development of late-onset anthracycline cardiomyopathy in mice<sup>5</sup> and may be so in humans.<sup>6</sup>

Female patients treated with anthracycline at puberty or adolescence are more susceptible to chronic anthracycline cardiotoxicity than male patients.<sup>7,8</sup> Anthracyclines do not accumulate in the adipose tissue; therefore, it has been postulated that their clearance is lower—and the concentrations reached in nonadipose organs, such as the heart, are higher—in female patients than in male patients with the same body surface area because the former have more fat mass than the latter.<sup>8</sup> Nevertheless, differences in the sex hormone milieu might also account for the predisposition of pubescent and adolescent girls to cardiac toxicity of anthracyclines. In fact, left ventricular function and survival following administration of doxorubicin, the prototype of anthracyclines, are significantly worse in mice knockout for the androgen

From the Laboratories of Cardiovascular Biology (P. Altieri, C. Barisione, E.L., G.P.B., M.C., P.S., C. Brunelli, and P. Ameri) and Cellular Therapies (A.G.), Department of Internal Medicine, and Regenerative Medicine, Department of Experimental Medicine (S.B.), University of Genova, Italy; Division of Internal Medicine, Department of Translational Medical Sciences, Federico II University, Napoli, Italy (C.G.T.).

**Correspondence to:** Pietro Ameri, MD, PhD, Laboratory of Cardiovascular Biology, Department of Internal Medicine, Room 117, Viale Benedetto XV, 6, 16132 Genova, Italy. E-mail: pietroameri@unige.it

Received July 9, 2015; accepted November 22, 2015.

© 2016 The Authors. Published on behalf of the American Heart Association, Inc., by Wiley Blackwell. This is an open access article under the terms of the Creative Commons Attribution-NonCommercial License, which permits use, distribution and reproduction in any medium, provided the original work is properly cited and is not used for commercial purposes.

receptor (AR) than in controls, pointing to a protective role of androgen against anthracycline cardiac damage.<sup>9</sup>

In this study, we compared the effect of testosterone and 17 $\beta$ -estradiol, the main androgen and estrogen, respectively, on an established cell model of doxorubicin-induced senescence of cardiomyocytes.<sup>10</sup> After finding that testosterone, but not 17 $\beta$ -estradiol, inhibited senescence elicited by doxorubicin, we sought to characterize the relevant signaling pathway.

## Methods

Unless otherwise indicated, all materials were supplied by Sigma-Aldrich.

## Animals

C57BL/6 breeders were purchased from Charles River Research Models and Services (Lecco, Italy) and housed in the animal facility of the IRCCS AOU San Martino—IST National Institute for Cancer Research in Genova, Italy. Primary mouse neonatal cardiomyocytes were isolated from the hearts of pups aged 2 days. Procedures complied with Italian national law concerning the use of animals for scientific purposes and were approved by the institutional animal care and use committee.

## Cell Culture and Experimental Design

Experiments were carried out with H9c2 cells, and then results were confirmed with neonatal cardiomyocytes.

The rat embryonic cardiac cell line H9c2 was purchased from the American Type Culture Collection (CRL-1446; Rockville, MD), cultured as reported previously,<sup>11</sup> and treated at a density of 70% to 80%. These cells express the male-specific gene sex-determining region Y (*SRY*) and have the testosterone metabolizing enzymes 5 $\alpha$ -reductase and aromatase.<sup>12</sup>

Primary cardiomyocytes were obtained as described previously, with minor modifications.<sup>13</sup> Briefly, hearts were harvested, digested overnight in a 0.06% (wt/vol) solution of trypsin (Gibco, Life Technologies), and further subjected to multiple digestions with a 0.1% type II collagenase solution (Worthington Biochemicals). Cells were preplated for 2 periods of 60 minutes each to enrich for cardiomyocytes and subsequently cultured in DMEM containing 4.5 g/L glucose supplemented with 10% FBS, 2 mmol/L L-glutamine, and 100 U/mL penicillin. Purity of the culture was routinely checked by immunofluorescence with a monoclonal anti-cardiac troponin T antibody (clone 13-11; Thermo Fisher Scientific), and each time at least 80% of cells were positive.

The complete culture medium was replaced with one with 0.5% FBS was added 1 hour before starting treatments, which

were also carried out in 0.5% FBS. Cells were exposed to 0.1  $\mu$ mol/L doxorubicin (Adriplastina; Pfizer) for 3 hours<sup>10</sup> with or without prior incubation with testosterone or 17 $\beta$ -estradiol for 15 minutes. Both hormones were preliminarily tested at different concentrations ranging from 0.1 to 1000 nmol/L (Figure 1). Testosterone was subsequently used at 10 nmol/L because this dose maximally reduced doxorubicin-induced senescence (Figure 1). Importantly, 10 nmol/L is within the normal values of circulating testosterone found in boys at puberty and adolescence.<sup>14</sup> In girls at the same age, physiological concentrations of 17 $\beta$ -estradiol are around 1 nmol/L.<sup>14</sup> Markers of senescence and telomere binding factor 2 (TRF2) levels were evaluated 45 hours after removing doxorubicin, whereas p53 was studied after 21 hours. The possibility of prolonged culturing of the H9c2 cell line was exploited to assess senescence over the long term. Cells were challenged with 0.1  $\mu$ mol/L doxorubicin as in short-term experiments but then were maintained in complete medium for 7, 14, or 21 days before determining senescence. Furthermore, the effect on senescence of a second 3-hour pulse of 0.1  $\mu$ mol/L doxorubicin, given 14 days after the first, was evaluated, as was the effect of preincubation with testosterone.

To identify the intracellular mediators of testosterone activity, cells were pretreated for 1 hour with the AR antagonist flutamide (10  $\mu$ mol/L), the phosphatidylinositol 3 kinase (PI3K) inhibitor LY294002 (20  $\mu$ mol/L; Calbiochem, Merck), the p38 MAPK inhibitor SB203580 (10  $\mu$ mol/L), and the JNK inhibitor SP600125 (20  $\mu$ mol/L); for 45 minutes with the nitric oxide synthase (NOS) inhibitor L-NG-nitroarginine methyl ester, L-NAME (1 mmol/L); or with relevant vehicles.

To analyze AKT and NOS-3 phosphorylation, cells were preincubated with testosterone or left untreated for 15 minutes followed by 20-minute exposure to doxorubicin or no treatment.

## Assessment of Senescence

Three different features of senescence were investigated, namely, enhanced  $\beta$ -galactosidase activity related to increased lysosomal content, formation of heterochromatin foci, and expression of the cell cycle inhibitor p16<sup>INK4a</sup>.<sup>15</sup> Staining for senescence-associated (SA)  $\beta$ -galactosidase was performed as described by Dimri et al,<sup>16</sup> and positive cells were counted out of total cells in 100 randomly chosen low-power fields ( $\times 100$ ). After staining for SA  $\beta$ -galactosidase, 0.13 mg/mL DAPI was added for 2 minutes at room temperature to costain for SA heterochromatin foci.<sup>17</sup> Immunocytochemistry for p16<sup>INK4a</sup> was carried out as described below. For each sample, images including a total of 300 cells were taken randomly and digitized at 256 levels of gray. The optical density of signals was measured with the Leica Q500 MC Image Analysis System.

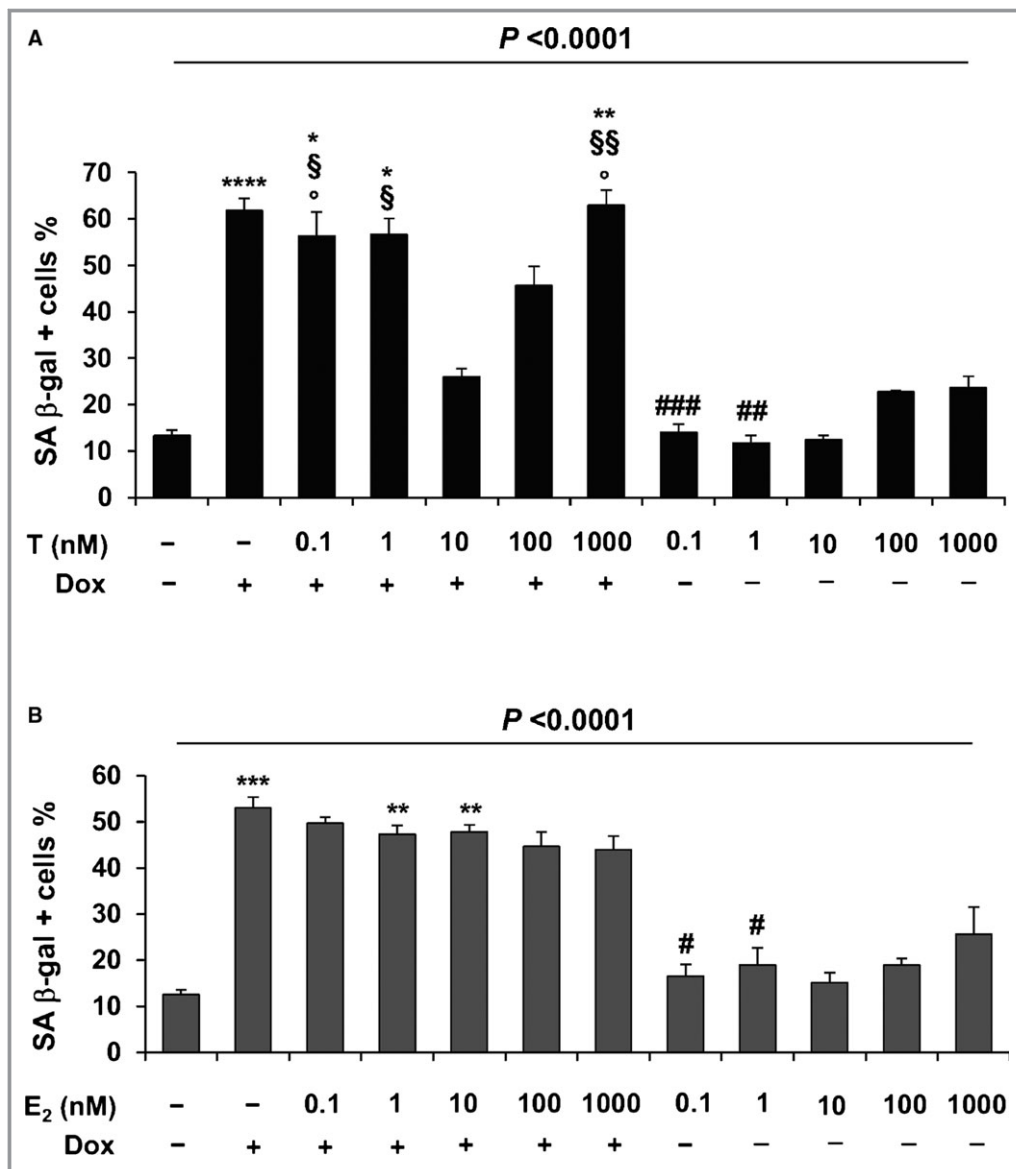


**Figure 1.** Effects of the studied concentrations of T and E<sub>2</sub> on Dox-induced senescence of H9c2 cells. Percentages (mean+SEM) of SA β-gal-positive H9c2 cells counted after no treatment or exposure to Dox with or without prior incubation with T (A) or E<sub>2</sub> (B) at the indicated concentrations. Group sizes: n=9 for no treatment, Dox, and any concentration of T or E<sub>2</sub> followed by Dox; n=6 for any concentration of T or E<sub>2</sub> tested alone. Kruskal–Wallis *P* values are presented above each graph. Dunn’s multiple comparisons test: \**P*<0.05, \*\**P*<0.01, \*\*\**P*<0.005, and \*\*\*\**P*<0.001 vs no treatment; #*P*<0.05, ##*P*<0.01, and ###*P*<0.005 vs Dox; \$*P*<0.05 and \$\$*P*<0.01 vs T0.1; °*P*<0.05 vs T1. Dox indicates doxorubicin; E<sub>2</sub>, 17β-estradiol; SA β-gal, senescence-associated β-galactosidase; T, testosterone.

### Western Blotting

Cells were lysed in lysis buffer (20 mmol/L Tris HCl [pH 7.5], 150 mmol/L NaCl, 1 mmol/L Na<sub>2</sub>-EDTA, 1 mmol/L EGTA, 1% NP40, 2.5 mmol/L Na<sub>2</sub>P<sub>2</sub>O<sub>7</sub>, and 1 mmol/L β-glycerophosphate). One mmol/L phenylmethylsulfonyl fluoride, 1 mmol/L Na<sub>3</sub>VO<sub>4</sub>, 1 mmol/L NaF, and a protease inhibitor cocktail (Thermo Fisher Scientific) were added to the buffer immediately before lysing.

The following primary antibodies were used (clones are indicated for monoclonal antibodies): anti-phosphorylated AKT (Ser<sup>473</sup>, clone D9E; Cell Signaling Technology), anti-phosphorylated AKT (Thr<sup>308</sup>), anti-AKT (H-136), anti-phosphorylated NOS-3 (Ser<sup>1177</sup>, 15E2; Santa Cruz Biotechnology), anti-NOS-3 (6H2; Cell Signaling Technology), anti-TRF2 (4S794.15; Imgenex, Novus Biologicals), anti-phosphorylated p53 (Ser<sup>15</sup>, D4S1H; Cell Signaling Technology), anti-p53, anti-GAPDH (FL-335), anti-AR (Millipore), and anti-ERK1/2. After

incubation with proper horseradish peroxidase–conjugated secondary antibody (Santa Cruz Biotechnology), bands were visualized with Clarity Western ECL Substrate (Bio-Rad) and quantified by densitometry using an image analysis system (UVItec). The quantity of phosphorylated AKT, NOS-3, and p53 was normalized for the amount of total protein. Levels of GAPDH and ERK1/2, respectively, were used to normalize the expression of TRF2 and p53 at 24 and 48 hours and the expression of AR at 7, 14, and 21 days.

## Immunocytochemistry

Cells were grown and treated on slides. At the end of experiments, they were fixed, permeabilized, and immunostained for p16<sup>INK4a</sup> with a specific rabbit primary antibody (Proteintech). Biotinylated secondary antibody (Vector), horseradish peroxidase–streptavidin (Vector), and 3,3'-diaminobenzidine (DAB Peroxidase Substrate Kit; Vector) were used to detect the bound primary antibody.<sup>18</sup>

## Statistical Analysis

Results are presented as mean±SEM of at least 3 independent replicates. Because of the small sample sizes, comparisons were drawn by Kruskal–Wallis followed by Dunn's multiple comparisons test. Statistical significance was set at  $P<0.05$ .

## Results

### Testosterone Protects H9c2 Cells Against Doxorubicin-Induced Senescence

The 3-hour treatment of H9c2 cells with doxorubicin significantly increased the percentage of senescent cells, as assessed by staining for SA  $\beta$ -galactosidase (Figure 2A and 2C), p16<sup>INK4a</sup> (Figure 2B and 2C), and SA heterochromatin foci (Figure 2D). Testosterone antagonized senescence elicited by doxorubicin (Figure 2A through 2C). In contrast, 17 $\beta$ -estradiol was not protective at either 100 nmol/L (Figure 2A through 2C), for which biologically relevant actions have been demonstrated,<sup>19</sup> or any concentration tested (Figure 1).

### Testosterone Inhibits Senescence Initiated by Doxorubicin Through an AR/PI3K/AKT/TRF2 Pathway

We reasoned that a rapid, nongenomic mode of action underlay the prevention of doxorubicin-triggered senescence by testosterone because it was achieved by pretreating H9c2 cells for just 15 minutes. In particular, AR has been shown to physically interact with PI3K, to enhance its activity, and to promote AKT phosphorylation.<sup>20,21</sup> Indeed, the AR antagonist

flutamide and the PI3K inhibitor LY294002 abrogated the reduction in cardiomyocyte senescence attained by testosterone (Figure 3). Conversely, the effect of testosterone was not influenced by inhibition of p38 and JNK (Figure 3), despite these kinases being involved in cardiomyocyte senescence caused by doxorubicin.<sup>10</sup> Western blotting demonstrated an increase in phosphorylation of AKT at both Ser<sup>473</sup> and Thr<sup>308</sup> in H9c2 cells incubated with testosterone or testosterone and then doxorubicin (Figure 4A through 4C).

Next we asked whether there was a link between the AR/PI3K/AKT signaling cascade activated by testosterone and TRF2. TRF2 is part of the telomere complex and contributes to maintenance of telomeric integrity and function and to suppression of the DNA damage response at the chromosome ends.<sup>22</sup> Our previous work identified its downregulation as a key event in the pathogenesis of doxorubicin-elicited cardiomyocyte senescence.<sup>10,23</sup> Doxorubicin also induces p53 phosphorylation and accumulation,<sup>24</sup> which also is involved in telomere dysfunction triggered by doxorubicin in cardiomyocytes.<sup>10</sup> We confirmed the reduction in TRF2 levels and the increase in those of phosphorylated and total p53 following incubation of H9c2 cells with doxorubicin and found that both alterations were prevented by testosterone (Figure 4D through 4F). The effect of testosterone on TRF2 was abolished by pretreatment with flutamide and LY294002 (Figure 4D through 4F), indicating that it was dependent on AR and PI3K.

### NOS-3 Is Implicated in Testosterone Prevention of Doxorubicin-Triggered Senescence and TRF2 Downregulation

Consistent with previous studies,<sup>20</sup> the activatory phosphorylation of NOS-3 at Ser<sup>1177</sup> increased in response to testosterone in H9c2 cells in a PI3K-dependent manner (Figure 5A). Because NOS-3<sup>-/-</sup> mice have lower levels of TRF2 than wild types,<sup>25</sup> we considered the possibility that NOS-3 was implicated in the signaling pathway linking testosterone to the modulation of TRF2 and senescence. Indeed, pretreatment of cells with the NOS inhibitor L-NAME reduced the ability of testosterone to prevent doxorubicin-induced TRF2 downregulation (Figure 5B) and senescence (Figure 5C).

### Confirmation of Results in Primary Neonatal Cardiomyocytes

Testosterone substantially reduced doxorubicin-caused senescence of primary mouse neonatal cardiomyocytes, whereas 17 $\beta$ -estradiol was only marginally effective (Figure 6A and 6C). Protection of testosterone was lost when cells were preincubated with flutamide, LY294002, or L-NAME but not with a p38 or JNK inhibitor (Figure 6B and 6C). Moreover, testosterone almost normalized the expression of

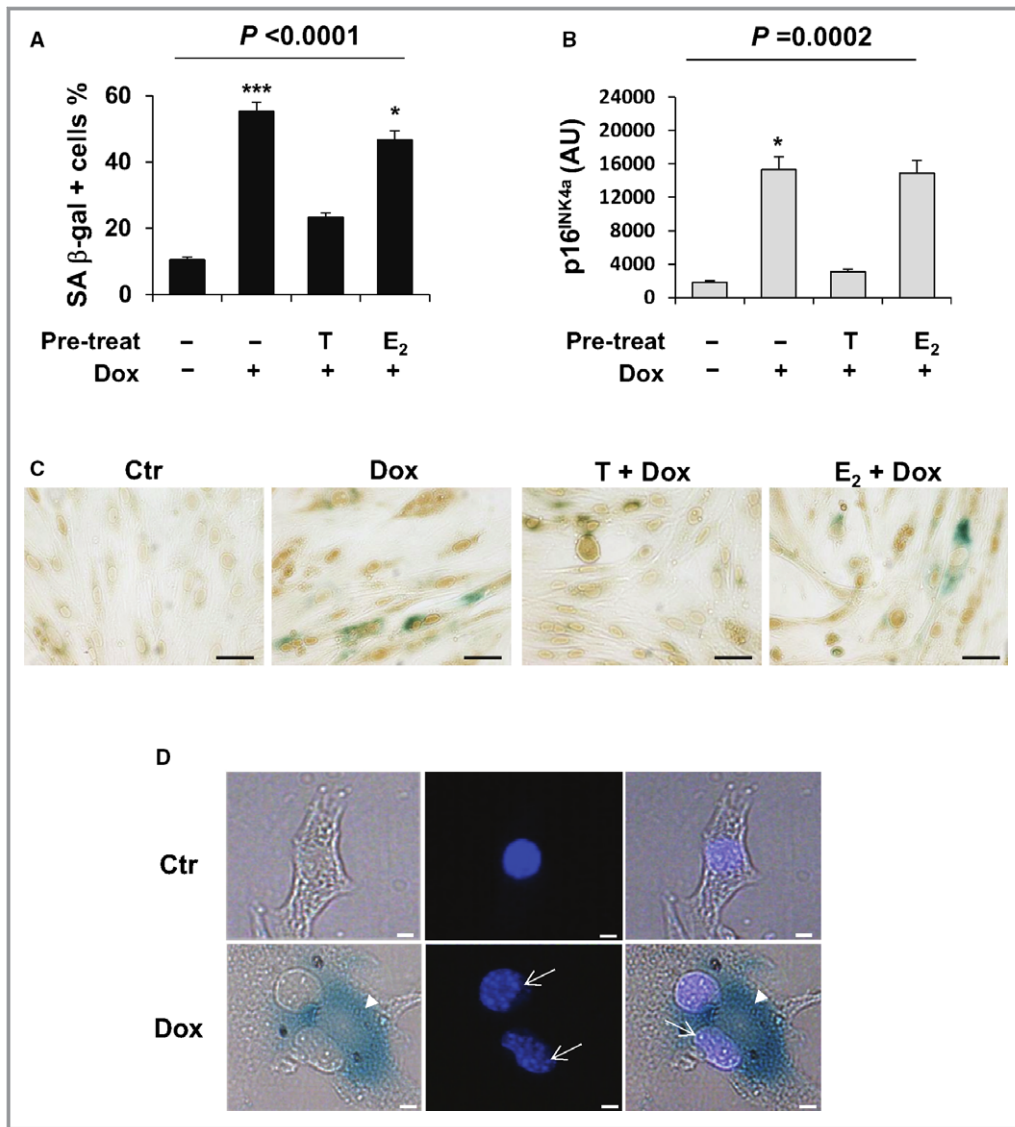


**Figure 2.** T prevents Dox-elicited senescence of H9c2 cells. A, Percentage of SA β-gal–positive H9c2 cells counted after no treatment or exposure to Dox with or without prior incubation with T or E<sub>2</sub>. B, Signal intensity quantification of the immunostaining for p16<sup>INK4a</sup> after the same treatments as in (A). C, Representative images of the costaining for p16<sup>INK4a</sup> (brown) and SA β-gal–positive (blue) cells. Magnification is ×400, and bars correspond to 50 μm. D, Representative pictures of Ctr or Dox-treated H9c2 cells costained for SA β-gal (cytoplasmic, arrowheads) and heterochromatin foci (dots within the nucleus, arrows). Magnification ×1000, bars 10 μm. Data in graphs are presented as means+SEM (7 and 4 observations for each SA β-gal and p16<sup>INK4a</sup> group, respectively); Kruskal–Wallis *P* values are shown on top. Dunn’s multiple comparisons test: \**P*<0.05 and \*\*\**P*<0.005 vs no treatment. AU indicates arbitrary units; Ctr, control; Dox, doxorubicin; E<sub>2</sub>, 17β-estradiol; SA β-gal, senescence-associated β-galactosidase; T, testosterone.

TRF2, and this effect was opposed by flutamide and LY294002 (Figure 6D).

### Testosterone Inhibition of Doxorubicin-Initiated Senescence is Long-Lasting

In agreement with our earlier findings,<sup>10</sup> the prosenescent response of H9c2 cardiomyoblasts to 3-hour treatment with doxorubicin persisted over time. After being challenged with

doxorubicin, cells proliferated more slowly and were passaged, on average, once a week compared with 2 or 3 times per week for control. In addition, a higher number of treated than control cells were positive for SA β-galactosidase after 7, 14, and 21 days (Figure 7A). Conversely, cells preincubated with testosterone and then exposed to doxorubicin were split twice a week and exhibited less SA β-galactosidase positivity than those treated with doxorubicin only, with this effect being AR dependent (Figure 7A).

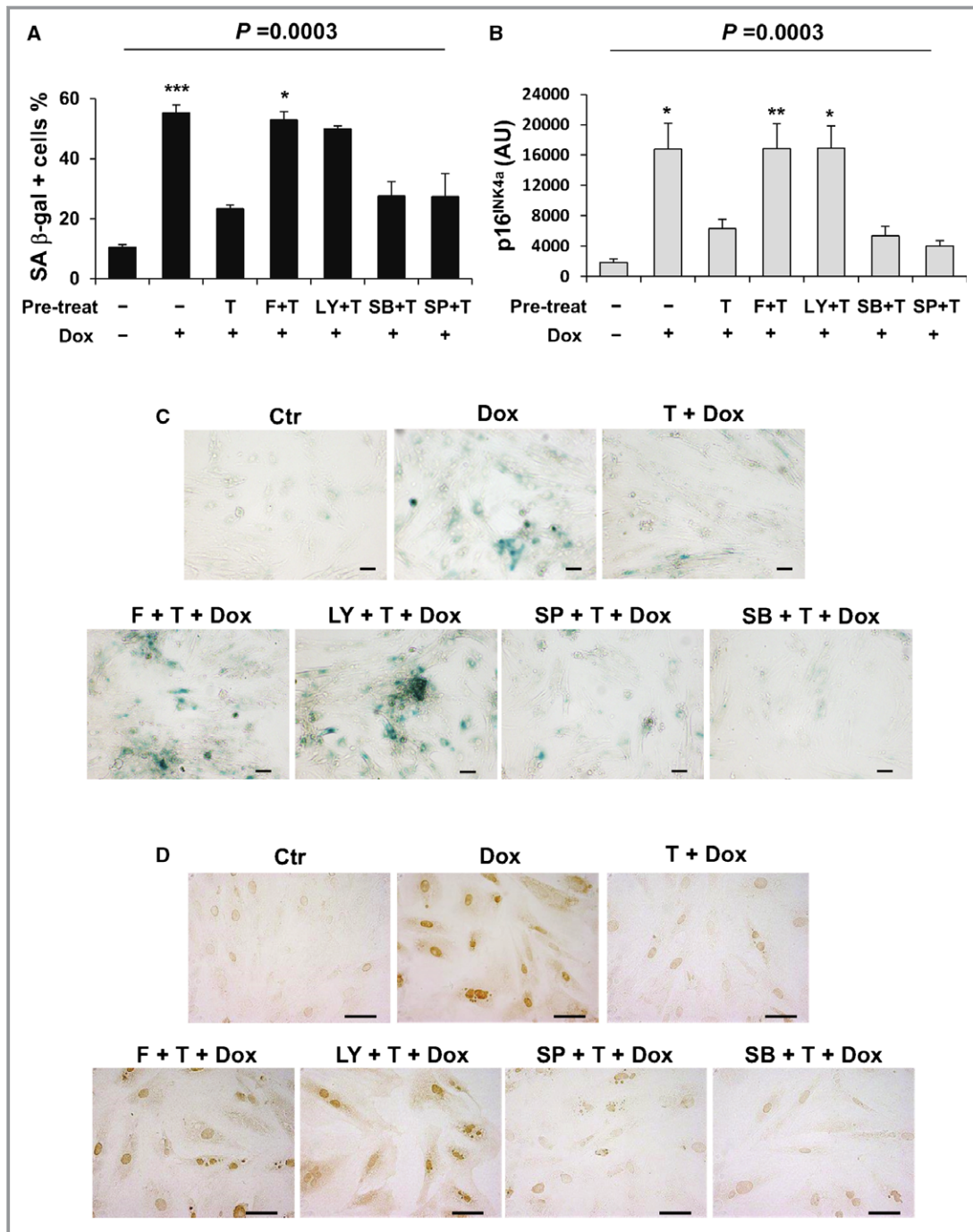


**Figure 3.** The androgen receptor/phosphatidylinositol 3 kinase/AKT pathway mediates T inhibition of Dox-induced senescence of H9c2 cardiomyoblasts. A, Percentage of SA β-galactosidase-positive H9c2 cells counted after no treatment or exposure to Dox with or without prior incubation with T, F and then T (F+T), LY and then T (LY+T), SB and then T (SB+T), or SP and then T (SP+T). B, Signal intensity quantification of the immunostaining for p16<sup>INK4a</sup> after the same treatments as in (A). C and D, Representative pictures of H9c2 cells stained for SA β-gal (C) and p16<sup>INK4a</sup> after no treatment or exposure to Dox with or without prior incubation with T, F and then T (F+T), LY and then T (LY+T), SB and then T (SB+T), or SP and then T (SP+T). Magnification is ×200 in (C) and ×400 in (D); bars correspond to 50 μm in both panels. Data in graphs are means±SEM (7 and 4 observations for each SA β-gal and p16<sup>INK4a</sup> group, respectively); P values are from Kruskal–Wallis test. Dunn’s multiple comparisons test: \*P<0.05, \*\*P<0.01, and \*\*\*P<0.005 vs no treatment. AU indicates arbitrary units; Ctr, control; Dox, doxorubicin; F, flutamide; LY, LY294002 (phosphatidylinositol 3 kinase inhibitor); SA β-gal, senescence-associated β-galactosidase; SB, SB203580 (p38 inhibitor); SP, SP600125 (JNK inhibitor); T, testosterone.

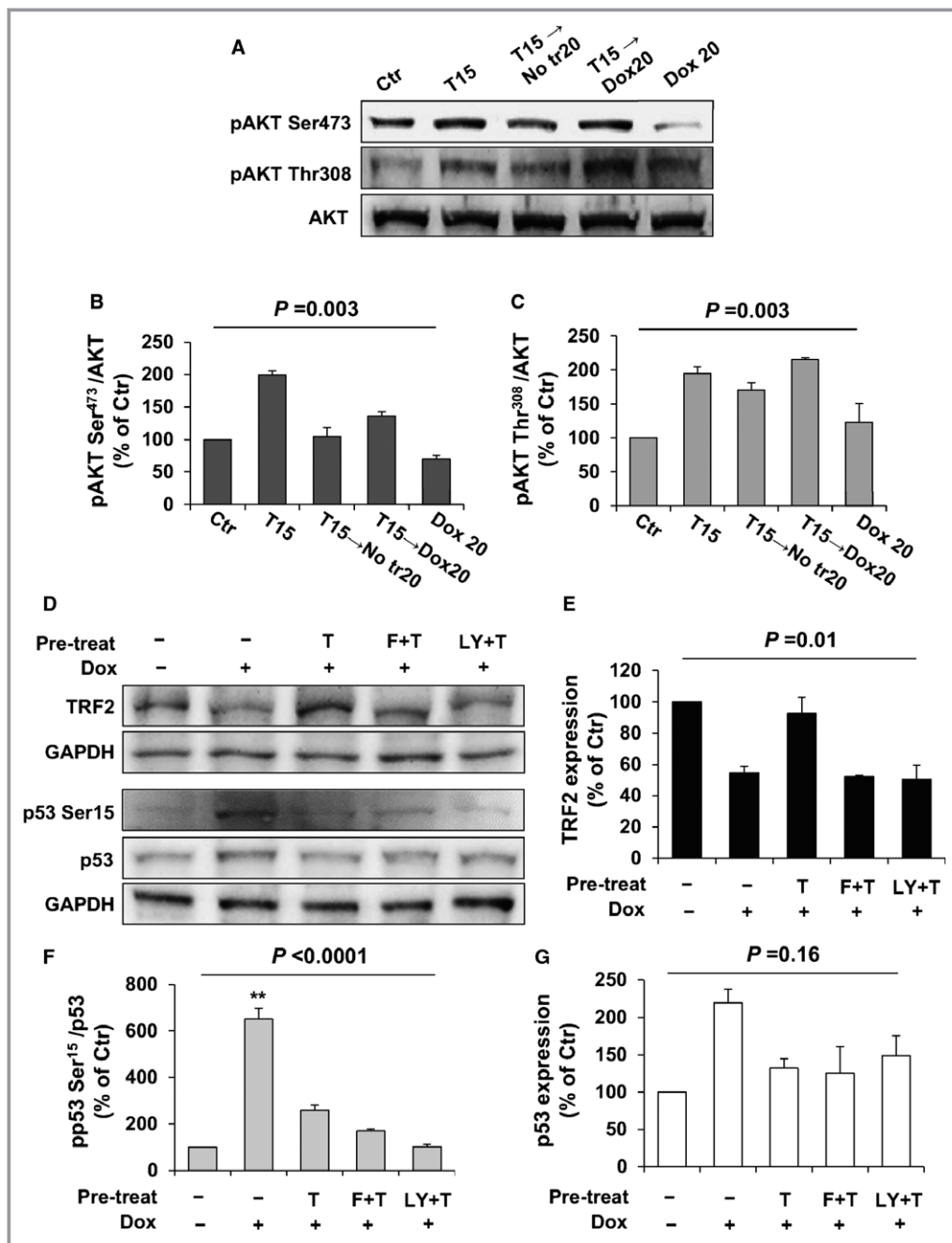


**Figure 4.** T stimulates AKT phosphorylation and prevents the changes in TRF2 and p53 levels caused by doxorubicin. A through C, Representative western blots (A) and band densitometry (B and C) for phosphorylated AKT in H9c2 cells preincubated with T or left untreated for 15 minutes followed by 20-minute exposure to Dox or no treatment. D through F, Representative western blots (D) and band densitometry (E through G) of TRF2 and p53 protein expression in H9c2 cells after no treatment or exposure to Dox with or without prior incubation with T, F and then T (F+T), or LY and then T (LY+T). Data are shown as means+SEM (3 observations per condition); P values are from Kruskal–Wallis test. Dunn’s multiple comparisons test: \*\*P<0.01 vs no treatment. Ctr indicates control; Dox, doxorubicin; F, flutamide; LY, LY294002 (phosphatidylinositol 3 kinase inhibitor); p, phosphorylated; T, testosterone; TRF2, telomere binding factor 2.

To further gain insight into the prolonged protection against doxorubicin cardiotoxicity conferred by testosterone, H9c2 cells were incubated with doxorubicin once or twice in

2 weeks, with or without being pretreated with testosterone. These experiments also allowed us to obtain data that were more easily translatable to the clinical setting, in which

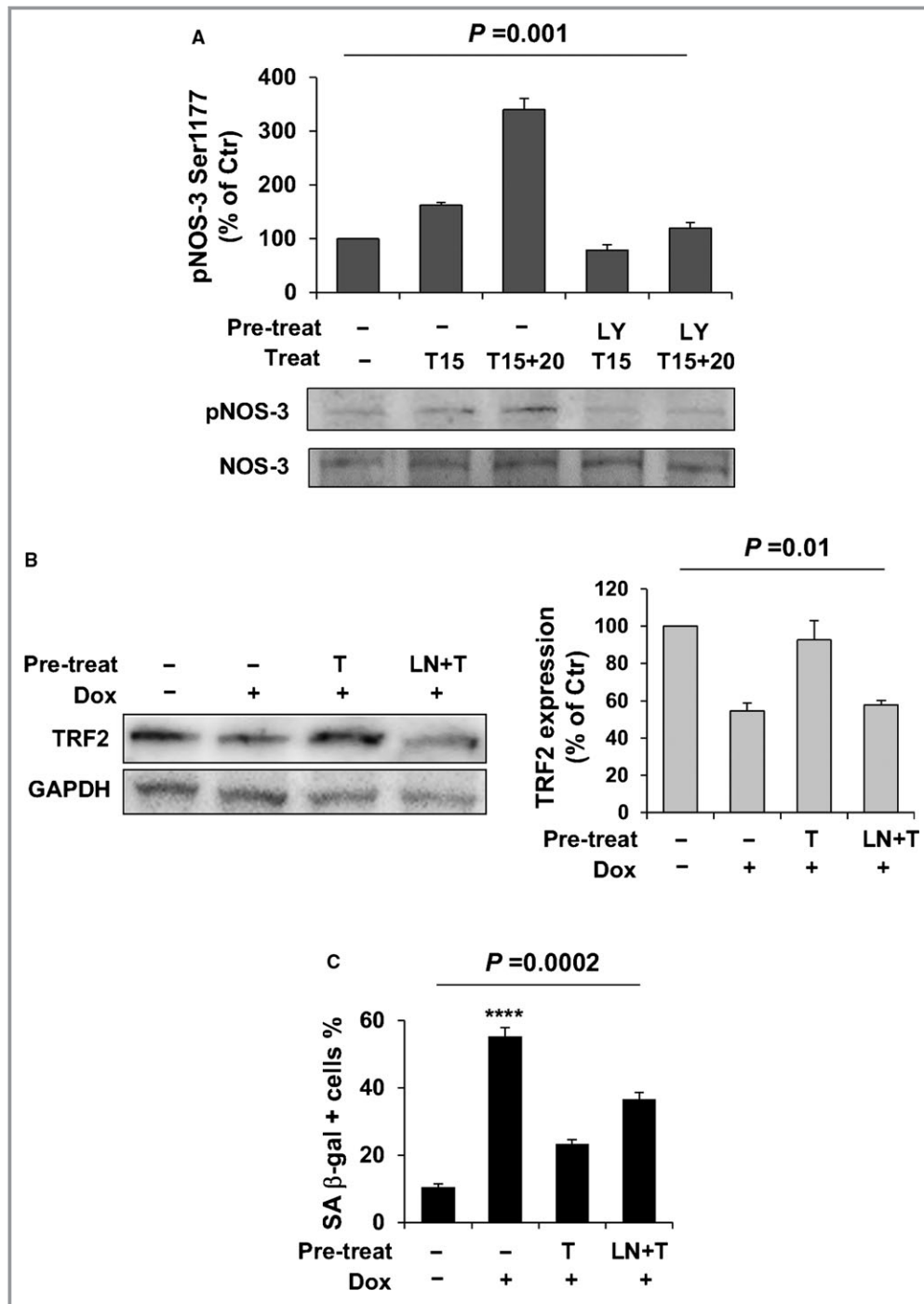


**Figure 5.** NOS-3 is implicated in testosterone prevention of Dox-triggered downregulation of TRF2 and senescence. A, Band densitometry and representative western blot for phosphorylated NOS-3 in H9c2 cells pretreated or not with LY and then incubated with T for 15 or 15+20 minutes, as indicated. B, Representative western blot and band densitometry of TRF2 protein expression in H9c2 cells after no treatment or exposure to Dox with or without prior incubation with T or LN and then T (LN+T). C, Percentage of SA β-galactosidase-positive H9c2 cells counted after the same treatments as in (B). Data are means±SEM. Western blot experiments included 3 replicates for each condition, whereas SA β-galactosidase was assessed 4 times for no treatment and Dox and 7 times for T or LN+T followed by Dox. Kruskal–Wallis  $P$  values are displayed above the graphs. Dunn’s multiple comparisons test: \*\*\*\* $P<0.001$  vs no treatment. Ctr indicates control; Dox, doxorubicin; LN, L-NG-nitroarginine methyl ester, or L-NAME; LY, LY294002 (phosphatidylinositol 3 kinase inhibitor); NOS, nitric oxide synthase; p, phosphorylated; SA β-gal, senescence-associated β-galactosidase; T, testosterone; TRF2, telomere binding factor 2.



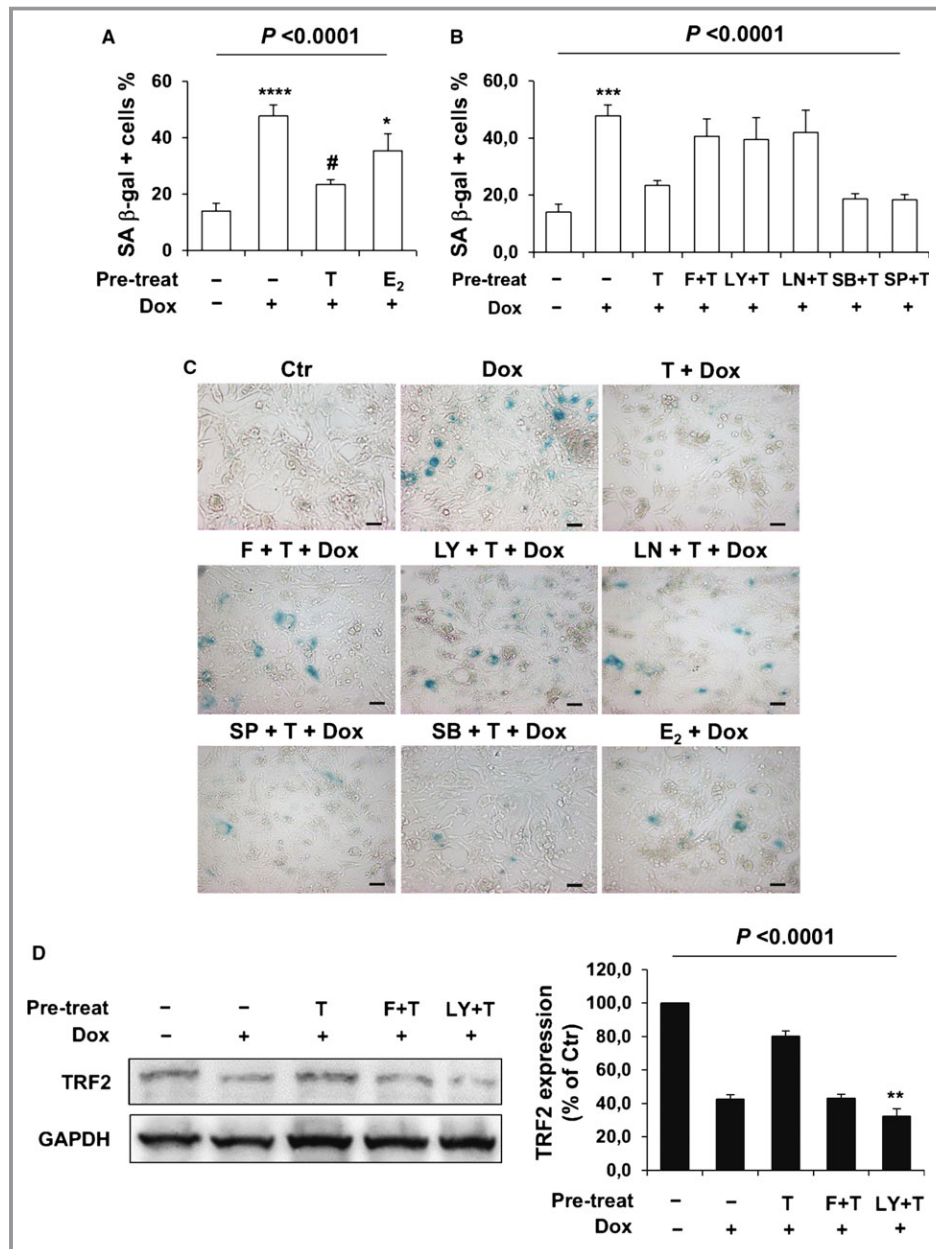


**Figure 6.** T inhibits Dox-caused senescence of primary neonatal cardiomyocytes via androgen receptor/phosphatidylinositol 3 kinase/nitric oxide synthase 3. A and B, Percentage of SA β-gal-positive primary mouse neonatal cardiomyocytes after no treatment or exposure to Dox with or without prior incubation with T or E<sub>2</sub> (A) or T, F and then T (F+T), LY and then T (LY+T), LN and then T (LN+T), SB and then T (SB+T), or SP and then T (SP+T) (B). C, Representative pictures of the staining for SA β-gal after the same treatments as in (A) and (B). Magnification is ×200, and bars correspond to 50 μm. D, Representative western blot and band densitometry of TRF2 protein expression in primary mouse neonatal cardiomyocytes after no treatment or exposure to Dox with or without prior incubation with T, F and then T (F+T), or LY and then T (LY+T). Means±SEM and Kruskal–Wallis *P* values are shown in graphs (western blots: 3 observations per group; SA β-gal: 7 assessments for no treatment, Dox, and T or E<sub>2</sub> followed by Dox; 4 for all the other conditions). Dunn’s multiple comparisons test: \**P*<0.05, \*\**P*<0.01, \*\*\**P*<0.005, and \*\*\*\**P*<0.001 vs no treatment; #*P*<0.05 vs Dox. Ctr indicates control; Dox, doxorubicin; E<sub>2</sub>, 17β-estradiol; F, flutamide; LN, L-NG-nitroarginine methyl ester, or L-NAME (nitric oxide synthase inhibitor); LY, LY294002 (phosphatidylinositol 3 kinase inhibitor); SA β-gal, senescence-associated β-galactosidase; SB, SB203580 (p38 inhibitor); SP, SP600125 (JNK inhibitor); T, testosterone; TRF2, telomere binding factor 2.

patients receive cycles of anthracycline-containing chemotherapy regimens every 2 or 3 weeks. Two pulses of doxorubicin 14 days apart caused senescence of H9c2 cardiomyoblasts in an additive manner (Figure 7B). Pretreatment with testosterone before each incubation with doxorubicin decreased the percentage of SA  $\beta$ -galactosidase-positive cells. Furthermore, senescence was reduced, albeit to a slightly lesser extent, when only the second pulse of doxorubicin was preceded by testosterone (Figure 7B). These results prompted us to investigate the expression of AR, which had proved to be necessary for testosterone action, over the 21 days of culturing. Surprisingly, and unlike observations at 24 and 48 hours (Figure 4D through 4F), GAPDH protein expression was substantially reduced by doxorubicin at 7, 14, and 21 days (Figure 8). Consequently, the expression of AR was normalized against that of ERK1/2, which did not vary throughout the experiment. At every time point, levels of AR were significantly lower in doxorubicin-treated cells than in control cells and were partially restored by preincubation with testosterone via AR (Figure 8).

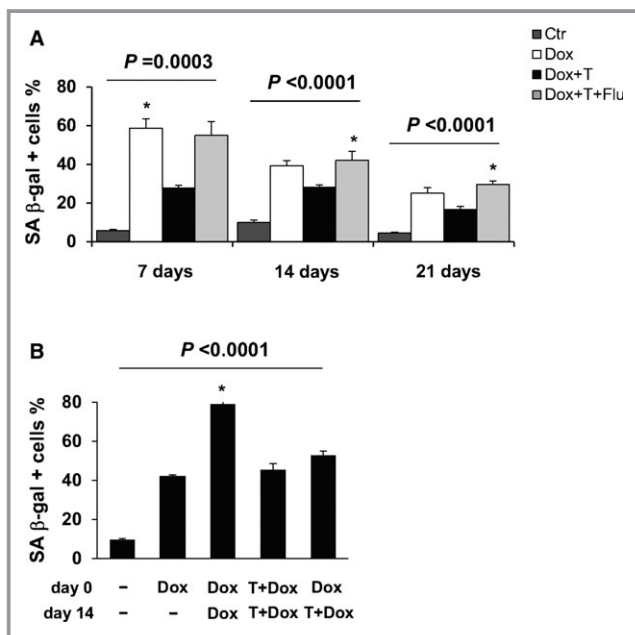


**Figure 7.** T protection against Dox-stimulated senescence is long-lasting. A, Percentage of SA  $\beta$ -gal-positive H9c2 cells counted 7, 14, and 21 days after no treatment or exposure to Dox, with or without prior incubation with T or F and then T (F+T). B, Percentage of SA  $\beta$ -gal-positive H9c2 cells counted after treating 15 days apart with Dox and/or T, as indicated. Graphs display means+SEM (5 observations per group) and Kruskal–Wallis *P* values. Dunn’s multiple comparisons test: \**P*<0.05 vs no treatment. Ctr indicates control; Dox, doxorubicin; F, flutamide; SA  $\beta$ -gal, senescence-associated  $\beta$ -galactosidase; T, testosterone.

## Discussion

Senescence of cardiac cells is considered to be of primary importance for the occurrence of anthracycline-related cardiomyopathy.<sup>26</sup> Doxorubicin induces a senescent-like phenotype in cardiomyocytes, with an abnormal pattern of troponin phosphorylation that may lead to inefficient cardiac contraction.<sup>4</sup> Moreover, doxorubicin causes senescence of resident cardiac progenitor cells (CPCs), which preserve myocardial tissue homeostasis following stress.<sup>27</sup> It has been proposed that senescence of CPCs in response to doxorubicin may be especially relevant at a young age because CPCs may no longer be able to activate a repair program for minor cardiac injuries, which therefore build up until they irreversibly affect cardiac structure and function.<sup>6</sup> In fact, mice injected with doxorubicin shortly after birth have normal hearts as adults but exhibit pathological eccentric hypertrophy following endurance training and more extensive myocardial infarction than wild-type littermates after coronary artery ligation, along with fewer, less proliferating, and less differentiating CPCs.<sup>5</sup>

In the present work, we found that testosterone antagonized doxorubicin-initiated senescence of both H9c2 cells and primary neonatal cardiomyocytes, whereas the effectiveness of 17 $\beta$ -estradiol was poor. This new information integrates the previous demonstration that AR deletion enhances cardiomyocyte apoptosis, cardiac remodeling, and mortality caused by doxorubicin in mice.<sup>9</sup> Moreover, it substantiates the hypothesis that differences in sex hormones may explain, at least in part, the higher risk of left ventricular dysfunction and heart failure that has been demonstrated in female survivors of cancer in puberty and adolescence who were treated with anthracycline.<sup>7,8,28</sup> It is possible that pharmacokinetic factors also contribute to the young female predisposition to anthracycline cardiotoxicity. The uptake of anthracyclines by adipose tissue is lower than by other organs.<sup>29</sup> Consequently, the higher the fat mass, the higher the concentration of anthracyclines in the bloodstream and in nonadipose tissues, including the heart.<sup>30,31</sup> Anthracyclines are dosed based on body surface area, but from puberty and thereafter, female patients generally have higher percentages of body fat than male patients, thus they might be more susceptible to cardiac side effects of anthracyclines.<sup>28</sup>

No clear sex difference in the incidence of anthracycline-related cardiotoxicity has been found in the adult oncological population. This may be due to the fact that anthracycline-based chemotherapies are most often given for breast cancer, which almost exclusive for the female sex. Nevertheless, the paradigm that androgen confers an advantage against cardiotoxicity of doxorubicin may be not valid in adulthood because estrogen during fertile age favorably influences cardiovascular risk factors and has direct beneficial activity on the heart.

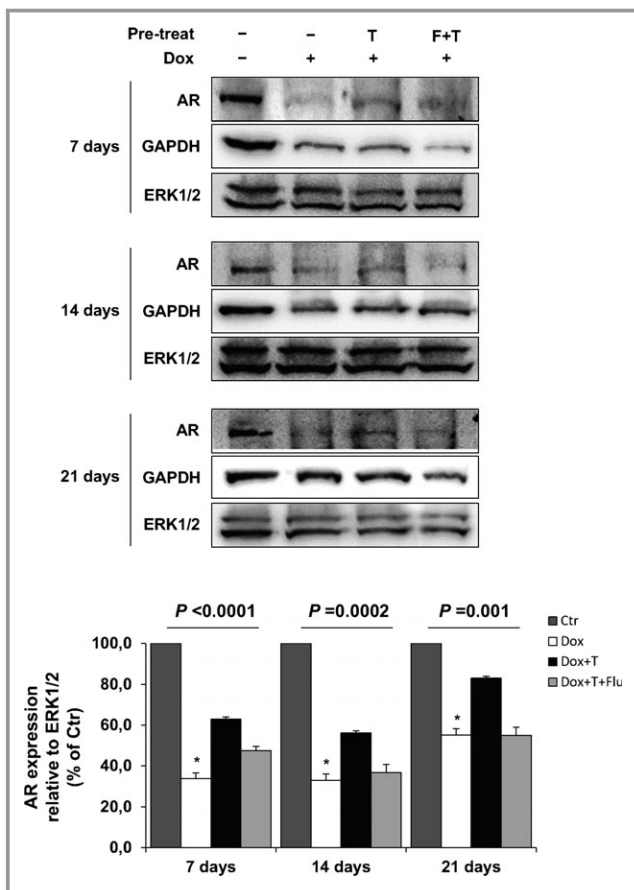


**Figure 8.** Effect of Dox on AR expression in H9c2 cells. Representative western blots and band densitometries (mean±SEM, 3 observations per group) of AR protein expression in H9c2 cells 7, 14, and 21 days after no treatment or exposure to Dox, with or without prior incubation with T or F and then T (F+T). Kruskal–Wallis  $P$  values are shown above each graph. Dunn's multiple comparisons test: \* $P < 0.05$  vs Ctr. AR indicates androgen receptor; Ctr, control; Dox, doxorubicin; F, flutamide; T, testosterone.

Telomere dysfunction is a well-established cause of senescence.<sup>32</sup> In a landmark paper, Maejima and colleagues showed that primary neonatal cardiomyocytes display markers of senescence and reduced telomerase activity on incubation with doxorubicin.<sup>4</sup> Expanding their observations, we previously demonstrated that TRF2 levels are decreased by treatment with doxorubicin and that silencing of *Terf2* is sufficient to trigger senescence in H9c2 cells and neonatal cardiomyocytes.<sup>10</sup> Subsequent studies have revealed that doxorubicin also induces senescence of vascular smooth muscle cells by downregulating TRF2.<sup>33</sup> In this study, it was shown that inhibition of doxorubicin-elicited senescence by testosterone is paralleled by the normalization of TRF2 expression, suggesting that prevention of TRF2 imbalance and telomeric dysfunction is at least 1 of the mechanisms by which testosterone counteracts cardiomyocyte senescence secondary to doxorubicin exposure.

Testosterone acts via AR, a steroid hormone receptor that classically works as a ligand-activated transcription factor, but it can also localize to the plasma membrane and initiate nongenomic signaling cascades.<sup>34</sup> In cardiomyocytes, this modality of action has already been reported, for example, for the modulation of intracellular calcium concentrations<sup>35</sup> and action potential duration<sup>20</sup> or for the stimulation of hypertrophy.<sup>36</sup> This study provides evidence that antagonism of doxorubicin-induced senescence and TRF2 downregulation is another nongenomic effect of testosterone and that it occurs through a signaling pathway involving PI3K, AKT, and NOS-3.

Activation of AKT has repeatedly been linked to inhibition of senescence in cardiovascular cells.<sup>25,37–40</sup> In addition, Ser<sup>473</sup> phosphorylation of AKT is decreased in senescent CPCs.<sup>41</sup> Interestingly, phosphorylation of AKT at this site has specifically been related to cardioprotection against doxorubicin, which is enhanced when PH domain leucine-rich repeat protein phosphatase 1, which selectively dephosphorylates AKT at Ser<sup>473</sup>, is knocked down.<sup>42</sup> Furthermore, AKT activation has been associated with TRF2 induction and PI3K or AKT inhibition with diminished TRF2 levels in endothelial cells.<sup>40</sup>

Based on the fact that NOS-3 is a downstream target of the AR/PI3K/AKT signal transduction cascade in cardiomyocytes<sup>20</sup> and on the finding that protection by testosterone was attenuated by pretreatment with L-NAME (Figure 5), we propose that NOS-3 mediates androgen modulation of TRF2 and antagonism of doxorubicin-stimulated senescence. In addition to the AR/PI3K/AKT/NOS-3 cascade, however, other nongenomic cascades may underlie testosterone regulation of TRF2 and senescence. Nitric oxide release by NOS-3, for example, has recently been demonstrated to reduce H<sub>2</sub>O<sub>2</sub>-induced senescence of H9c2 cells by improving redox state.<sup>43</sup>

In apparent discordance with our results, mice knockout for *NOS3* are less sensitive to doxorubicin-triggered cardiac cell apoptosis, intramyocardial production of reactive oxygen species, left ventricular dysfunction, and death. Furthermore, cardiomyocyte-specific overexpression of *NOS3* exacerbates cardiac toxicity of doxorubicin.<sup>44,45</sup> This phenotype has been ascribed to the involvement of NOS-3 in the so-called redox cycling of anthracyclines, namely, the reduction to semiquinone radicals that then react with oxygen and undergo oxidation with generation of superoxide anion. In contrast, another NOS isozyme, NOS-1, is overexpressed in NOS-3 knockouts, and it has been suggested that NOS-1 might actually be responsible for the resistance to doxorubicin cardiac damage associated with *NOS3* deletion.<sup>45</sup> Consequently, NOS activity may be generally protective against doxorubicin cardiotoxicity although with differences in the involved isoform, depending on the experimental model.

We observed the most intense decrease in doxorubicin-initiated senescence of cardiomyocytes with 10 nmol/L

testosterone, which is well within the range of normal plasma values for pubescent and adolescent boys.<sup>14</sup> Inhibition of senescence was not as strong with 100 nmol/L, a supra-physiological concentration of testosterone,<sup>14</sup> and was lost with 1000 nmol/L testosterone, which is a very high dose. This latter dose may no longer be able to activate antisenesescence pathways, similar to what has been reported previously for the modulation of calcium transients by testosterone,<sup>35</sup> or it may stimulate signaling cascades that oppose those preventing doxorubicin-induced senescence. In any case, it should be noted that important variations in doxorubicin and testosterone metabolism and action likely exist between cell cultures and the whole human body.

In our experiments, doxorubicin after testosterone differently influenced the phosphorylation status of Ser<sup>473</sup> and Thr<sup>308</sup> of AKT. There are several possible reasons for this phenomenon, including doxorubicin modulation of the activity of AKT kinases and phosphatases and of the interaction between AKT and its binding proteins. Nevertheless, it should be kept in mind that the effect of doxorubicin on AKT phosphorylation appears to be importantly affected by the experimental setting, up to the point that opposite results have been obtained with the same animal model.<sup>46,47</sup>

Doxorubicin persistently downregulated AR protein in H9c2 cardiomyoblasts, and pretreatment with testosterone partially rescued its expression, possibly allowing androgen contained in the culture medium to antagonize senescence triggered by doxorubicin. Strikingly, a reduction in GAPDH protein expression was also observed during prolonged culturing. It is known that doxorubicin causes profound posttranslational modifications to proteins,<sup>48</sup> among which may be AR and GAPDH. Nonetheless, this is speculation, and future investigations are needed to characterize the modulation of AR and GAPDH by doxorubicin and the mechanism behind it.

The present study has limitations that must be acknowledged. First, it is possible that androgen is also protective against doxorubicin-initiated senescence via canonical genomic pathways, and this was not addressed by our experiments. Similarly, it cannot be excluded that 17 $\beta$ -estradiol also promotes the transcription of genes that counteract doxorubicin toxicity and/or senescence. Second, doxorubicin affects many other cellular events that have been not analyzed in this study, such as apoptosis and autophagy, and that might be influenced by sex hormones. Third, further studies specifically using CPCs are needed because they are thought to be pivotal in anthracycline cardiotoxicity. Finally, it remains to be proven in vivo that inhibition of cardiomyocyte and possibly CPC senescence by testosterone actually translates into reduced incidence or severity of anthracycline cardiomyopathy.

In conclusion, this work offers a biological explanation for the relative resistance of the male heart to anthracycline

toxicity. In general, it adds to the knowledge of the cardiovascular effects of testosterone and may form the basis for additional research into the role of this hormone in stress-induced senescence of cardiac cells.

## Acknowledgments

The authors acknowledge Dr Barbara Rebesco, Director of the Antitubercular Drug Unit, IRCCS AOU San Martino—IST National Institute for Cancer Research, Genova, Italy, for providing doxorubicin.

## Sources of Funding

This work was partially supported by a grant funded by the University of Genova to Pietro Ameri (Progetto di Ricerca d'Ateneo 2014).

## Disclosures

None.

## References

1. Yeh ET, Bickford CL. Cardiovascular complications of cancer therapy: incidence, pathogenesis, diagnosis, and management. *J Am Coll Cardiol*. 2009;53:2231–2247.
2. Hahn VS, Lenihan DJ, Ky B. Cancer therapy-induced cardiotoxicity: basic mechanisms and potential cardioprotective therapies. *J Am Heart Assoc*. 2014;3:e000665 doi: 10.1161/JAHA.113.000665.
3. Tocchetti CG, Carpi A, Coppola C, Quintavalle C, Rea D, Campesan M, Arcari A, Piscopo G, Cipresso C, Monti MG, De Lorenzo C, Arra C, Condorelli G, Di Lisa F, Maurea N. Ranolazine protects from doxorubicin-induced oxidative stress and cardiac dysfunction. *Eur J Heart Fail*. 2014;16:358–366.
4. Maejima Y, Adachi S, Ito H, Hirao K, Isobe M. Induction of premature senescence in cardiomyocytes by doxorubicin as a novel mechanism of myocardial damage. *Aging Cell*. 2008;7:125–136.
5. Huang C, Zhang X, Ramil JM, Rikka S, Kim L, Lee Y, Gude NA, Thistlethwaite PA, Sussman MA, Gottlieb RA, Gustafsson AB. Juvenile exposure to anthracyclines impairs cardiac progenitor cell function and vascularization resulting in greater susceptibility to stress-induced myocardial injury in adult mice. *Circulation*. 2010;121:675–683.
6. Piegari E, De Angelis A, Cappetta D, Russo R, Esposito G, Costantino S, Graiani G, Frati C, Prezioso L, Berrino L, Urbaneck K, Quaini F, Rossi F. Doxorubicin induces senescence and impairs function of human cardiac progenitor cells. *Basic Res Cardiol*. 2013;108:334.
7. Green DM, Grigoriev YA, Nan B, Takashima JR, Norkool PA, D'Angio GJ, Breslow NE. Congestive heart failure after treatment for Wilms' tumor: a report from the National Wilms' Tumor Study group. *J Clin Oncol*. 2001;19:1926–1934.
8. Lipshultz SE, Lipsitz SR, Mone SM, Goorin AM, Sallan SE, Sanders SP, Orav EJ, Gelber RD, Colan SD. Female sex and drug dose as risk factors for late cardiotoxic effects of doxorubicin therapy for childhood cancer. *N Engl J Med*. 1995;332:1738–1743.
9. Ikeda Y, Aihara K, Akaike M, Sato T, Ishikawa K, Ise T, Yagi S, Iwase T, Ueda Y, Yoshida S, Azuma H, Walsh K, Tamaki T, Kato S, Matsumoto T. Androgen receptor counteracts Doxorubicin-induced cardiotoxicity in male mice. *Mol Endocrinol*. 2010;24:1338–1348.
10. Spallarossa P, Altieri P, Aloï C, Garibaldi S, Barisione C, Ghigliotti G, Fugazza G, Barsotti A, Brunelli C. Doxorubicin induces senescence or apoptosis in rat neonatal cardiomyocytes by regulating the expression levels of the telomere binding factors 1 and 2. *Am J Physiol Heart Circ Physiol*. 2009;297:H2169–H218.
11. Spallarossa P, Altieri P, Garibaldi S, Ghigliotti G, Barisione C, Manca V, Fabbi P, Ballestrero A, Brunelli C, Barsotti A. Matrix metalloproteinase-2 and -9 are induced differently by doxorubicin in H9c2 cells: the role of MAP kinases and NAD(P)H oxidase. *Cardiovasc Res*. 2006;69:736–745.

12. Ballantyne T, Du Q, Jovanović S, Neemo A, Holmes R, Sinha S, Jovanović A. Testosterone protects female embryonic heart H9c2 cells against severe metabolic stress by activating estrogen receptors and up-regulating IES SUR2B. *Int J Biochem Cell Biol*. 2013;45:283–291.
13. Radisic M, Park H, Shing H, Consi T, Schoen FJ, Langer R, Freed LE, Vunjak-Novakovic G. Functional assembly of engineered myocardium by electrical stimulation of cardiac myocytes cultured on scaffolds. *Proc Natl Acad Sci USA*. 2004;101:18129–18134.
14. Konforte D, Shea JL, Kyriakopoulou L, Colantonio D, Cohen AH, Shaw J, Bailey D, Chan MK, Armbruster D, Adeli K. Complex biological pattern of fertility hormones in children and adolescents: a study of healthy children from the CALIPER cohort and establishment of pediatric reference intervals. *Clin Chem*. 2013;59:1215–1227.
15. Bernardes de Jesus B, Blasco MA. Assessing cell and organ senescence biomarkers. *Circ Res*. 2012;111:97–109.
16. Dimiri GP, Lee X, Basile G, Acosta M, Scott G, Roskelley C, Medrano EE, Linskens M, Rubelj I, Pereira-Smith O. A biomarker that identifies senescent human cells in culture and in aging skin in vivo. *Proc Natl Acad Sci USA*. 1995;92:9363–9367.
17. Zhang R, Poustovoitov MV, Ye X, Santos HA, Chen W, Daganzo SM, Erzberger JP, Serebriiskii IG, Canutescu AA, Dunbrack RL, Pehrson JR, Berger JM, Kaufman PD, Adams PD. Formation of MacroH2A-containing senescence-associated heterochromatin foci and senescence driven by ASF1a and HIRA. *Dev Cell*. 2005;8:19–30.
18. Verzola D, Gandolfo MT, Salvatore F, Villaggio B, Gianiorio F, Traverso P, Deferrari G, Garibotto G. Testosterone promotes apoptotic damage in human renal tubular cells. *Kidney Int*. 2004;65:1252–1264.
19. Harvey PA, Leinwand LA. Oestrogen enhances cardiotoxicity induced by Sunitinib by regulation of drug transport and metabolism. *Cardiovasc Res*. 2015;107:66–77.
20. Bai CX, Kurokawa J, Tamagawa M, Nakaya H, Furukawa T. Nontranscriptional regulation of cardiac repolarization currents by testosterone. *Circulation*. 2005;112:1701–1710.
21. Baron S, Manin M, Beaudoin C, Leotoing L, Communal Y, Veyssiere G, Morel L. Androgen receptor mediates non-genomic activation of phosphatidylinositol 3-OH kinase in androgen-sensitive epithelial cells. *J Biol Chem*. 2004;279:14579–14586.
22. De Boeck G, Forsyth RG, Praet M, Hogendoorn PC. Telomere-associated proteins: cross-talk between telomere maintenance and telomere-lengthening mechanisms. *J Pathol*. 2009;217:327–344.
23. Altieri P, Spallarossa P, Barisione C, Garibaldi S, Garuti A, Fabbi P, Ghigliotti G, Brunelli C. Inhibition of doxorubicin-induced senescence by PPAR $\delta$  activation agonists in cardiac muscle cells: cooperation between PPAR $\delta$  and Bcl6. *PLoS One*. 2012;7:e46126.
24. Liu J, Mao W, Ding B, Liang CS. ERKs/p53 signal transduction pathway is involved in doxorubicin-induced apoptosis in H9c2 cells and cardiomyocytes. *Am J Physiol Heart Circ Physiol*. 2008;295:H1956–H1965.
25. Werner C, Hanhoun M, Widmann T, Kazakov A, Semenov A, Pöss J, Bauersachs J, Thum T, Pfreundschuh M, Müller P, Haendeler J, Böhm M, Laufs U. Effects of physical exercise on myocardial telomere-regulating proteins, survival pathways, and apoptosis. *J Am Coll Cardiol*. 2008;52:470–482.
26. De Angelis A, Piegari E, Cappetta D, Marino L, Filippelli A, Berrino L, Ferreira-Martins J, Zheng H, Hosoda T, Rota M, Urbanek K, Kajstura J, Leri A, Rossi F, Anversa P. Anthracycline cardiomyopathy is mediated by depletion of the cardiac stem cell pool and is rescued by restoration of progenitor cell function. *Circulation*. 2010;121:276–292.
27. Bollini S, Smart N, Riley PR. Resident cardiac progenitor cells: at the heart of regeneration. *J Mol Cell Cardiol*. 2011;50:296–303.
28. Lipshultz SE, Sambatakos P, Maguire M, Karnik R, Ross SW, Franco VI, Miller TL. Cardiotoxicity and cardioprotection in childhood cancer. *Acta Haematol*. 2014;132:391–399.
29. Lee YT, Chan KK, Harris PA, Cohen JL. Distribution of adriamycin in cancer patients: tissue uptakes, plasma concentration after IV and hepatic IA administration. *Cancer*. 1980;45:2231–2239.
30. Rodvold KA, Rushing DA, Tewksbury DA. Doxorubicin clearance in the obese. *J Clin Oncol*. 1988;6:1321–1327.
31. Thompson PA, Rosner GL, Matthey KK, Moore TB, Bomgaars LR, Ellis KJ, Renbarger J, Berg SL. Impact of body composition on pharmacokinetics of doxorubicin in children: a Glaser Pediatric Research Network study. *Cancer Chemother Pharmacol*. 2009;64:243–251.
32. Lechel A, Satyanarayana A, Ju Z, Plentz RR, Schaezlein S, Rudolph C, Wilkens L, Wiemann SU, Saretzki G, Malek NP, Manns MP, Buer J, Rudolph KL. The cellular level of telomere dysfunction determines induction of senescence or apoptosis in vivo. *EMBO Rep*. 2005;6:275–281.
33. Hodjat M, Haller H, Dumler I, Kiyan Y. Urokinase receptor mediates doxorubicin-induced vascular smooth muscle cell senescence via proteasomal degradation of TRF2. *J Vasc Res*. 2013;50:109–123.
34. Michels G, Hoppe UC. Rapid actions of androgens. *Front Neuroendocrinol*. 2008;29:182–198.
35. Vicencio JM, Ibarra C, Estrada M, Chiong M, Soto D, Parra V, Diaz-Araya G, Jaimovich E, Lavandero S. Testosterone induces an intracellular calcium increase by a nongenomic mechanism in cultured rat cardiac myocytes. *Endocrinology*. 2006;147:1386–1395.
36. Altamirano F, Oyarce C, Silva P, Toyos M, Wilson C, Lavandero S, Uhlén P, Estrada M. Testosterone induces cardiomyocyte hypertrophy through mammalian target of rapamycin complex 1 pathway. *J Endocrinol*. 2009;202:299–307.
37. D'Amario D, Cabral-Da-Silva MC, Zheng H, Fiorini C, Goichberg P, Steadman E, Ferreira-Martins J, Sanada F, Piccoli M, Cappetta D, D'Alessandro DA, Michler RE, Hosoda T, Anastasia L, Rota M, Leri A, Anversa P, Kajstura J. Insulin-like growth factor-1 receptor identifies a pool of human cardiac stem cells with superior therapeutic potential for myocardial regeneration. *Circ Res*. 2011;108:1467–1481.
38. Thum T, Hoerber S, Froese S, Klink I, Stichtenoth DO, Galuppo P, Jakob M, Tsikas D, Anker SD, Poole-Wilson PA, Borlak J, Ertl G, Bauersachs J. Age-dependent impairment of endothelial progenitor cells is corrected by growth-hormone-mediated increase of insulin-like growth-factor-1. *Circ Res*. 2007;100:434–443.
39. Torella D, Rota M, Nurzynska D, Musso E, Monsen A, Shiraishi I, Zias E, Walsh K, Rosenzweig A, Sussman MA, Urbanek K, Nadal-Ginard B, Kajstura J, Anversa P, Leri A. Cardiac stem cell and myocyte aging, heart failure, and insulin-like growth factor-1 overexpression. *Circ Res*. 2004;94:514–524.
40. Werner C, Gensch C, Pöss J, Haendeler J, Böhm M, Laufs U. Pioglitazone activates aortic telomerase and prevents stress-induced endothelial apoptosis. *Atherosclerosis*. 2011;216:23–34.
41. Avolio E, Gianfranceschi G, Cesselli D, Caragnano A, Athanasakis E, Katare R, Meloni M, Palma A, Barchiesi A, Vascotto C, Toffoletto B, Mazzega E, Finato N, Aresu G, Livi U, Emanuelli C, Scoles G, Beltrami CA, Madeddu P, Beltrami AP. Ex vivo molecular rejuvenation improves the therapeutic activity of senescent human cardiac stem cells in a mouse model of myocardial infarction. *Stem Cells*. 2014;32:2373–2385.
42. Miyamoto S, Purcell NH, Smith JM, Gao T, Whittaker R, Huang K, Castillo R, Glembocki CC, Sussman MA, Newton AC, Brown JH. PHLPP-1 negatively regulates Akt activity and survival in the heart. *Circ Res*. 2010;107:476–484.
43. Dong R, Xu X, Li G, Feng W, Zhao G, Zhao J, Wang DW, Tu L. Bradykinin inhibits oxidative stress-induced cardiomyocytes senescence via regulating redox state. *PLoS One*. 2013;8:e77034.
44. Neilan TG, Blake SL, Ichinose F, Raheer MJ, Buys ES, Jassal DS, Furutani E, Perez-Sanz TM, Graveline A, Janssens SP, Picard MH, Scherrer-Crosbie M, Bloch KD. Disruption of nitric oxide synthase 3 protects against the cardiac injury, dysfunction, and mortality induced by doxorubicin. *Circulation*. 2007;116:506–514.
45. Deng S, Kruger A, Schmidt A, Metzger A, Yan T, Gödtel-Armbrust U, Hasenfuss G, Brunner F, Wojnowski L. Differential roles of nitric oxide synthase isozymes in cardiotoxicity and mortality following chronic doxorubicin treatment in mice. *Naunyn Schmiedeberg Arch Pharmacol*. 2009;380:25–34.
46. Gabrielson K, Bedja D, Pin S, Tsao A, Gama L, Yuan B, Muratore N. Heat shock protein 90 and ErbB2 in the cardiac response to doxorubicin injury. *Cancer Res*. 2007;67:1436–1441.
47. Xiang P, Deng HY, Li K, Huang GY, Chen Y, Tu L, Ng PC, Pong NH, Zhao H, Zhang L, Sung RY. Dexrazoxane protects against doxorubicin-induced cardiomyopathy: upregulation of Akt and Erk phosphorylation in a rat model. *Cancer Chemother Pharmacol*. 2009;63:343–349.
48. Aryal B, Jeong J, Rao VA. Doxorubicin-induced carbonylation and degradation of cardiac myosin binding protein C promote cardiotoxicity. *Proc Natl Acad Sci USA*. 2014;111:2011–2016.